A New Failure Criterion for Woven-roving GFRE Thick Tube Subjected to Combined Fatigue Bending Moments and Internal hydrostatic Pressure

M.N. Abouelwafa, H.A. El-Gamal, Y. S. Mohamed and Wael A. Al-Tabey

Abstract—Choosing the suitable failure criterion represents the main target for many researchers working with materials, and it represents the first step for new materials before being used in the field. Considering composite materials, specifically, makes it more challenging, because of their very special behavior and characteristics. Besides, it must be noted that, the suitability of a certain criterion differs greatly according to the tested material, and its stress state. Thick-walled tubular specimens, made from woven-roving Glass Fiber-Reinforced Epoxy (GFRE) with two fiber orientations, $[0°,90°]_{3s}$ and $[\pm45°]_{3s}$, and two manufacture methods M_1 and M_2 to prepare the test specimens, were tested under combined fatigue bending and Internal hydrostatic Pressure at different pressure ratios (P_r), $P_r = 0, 0.25, 0.5, 0.75$ (i.e. pressures amounting to 0%, 25%, 50% and 75% of the burst pressure). The $[0°,90°]_{3s}$ specimens were found to have higher bending strength than the $[\pm45°]_{3s}$ specimens, at all pressure ratios; This is due to the fiber orientation $[0°,90°]_{3s}$ has a minimum value of stress component σ6 which equal to zero. For both fiber orientations $[0°,90°]_{3s}$ and $[\pm45°]_{3s}$ and both manufacture methods M_1 and M_2, were found none of the available criteria succeeded in predicting failure for the studied case, this due to the effect of hoop stress on values of amplitude component and the corresponding fatigue strength; consequently. A new modifying term was introduced that made Norris-Distortional, Tsai-Hahn, and Tsai-Hill criteria suitable for this studied case, resulting in a new criterion.

Keywords—Failure criterion; Hoop Stress; Bending Fatigue; internal hydrostatic pressure; Reinforced Epoxy; composite thick tube; multilayer.

1. Introduction

The simplified failure envelopes for composite materials are not derived from physical theories of failure, in which the actual physical processes that cause failure on a microscopic level are integrated to obtain a failure theory. However the phenomenological theories in which the actual failure mechanisms are dealed with for composite materials. The concentration in this case is on the gross macroscopic events of failure.

Phenomenological theories are based on curve fitting, so they are failure criteria and not theories of any kind (the term theory implies a formal derivation process). Unfortunately, with curve fitting the ability to determine the failure mode is lost. That is, curve-fit failure criteria are generally disassociated with knowledge of precisely how the material fails. Only the occurrence of failure is predicted and not the actual mode of failure. For conventional engineering metals, the curve fitting process process is less challenged for metals than for orthotropic materials because metals are isotropic, so they do not have same strength in different directions [1].

- *M.N. Abouelwafa, H.A. El-Gamal, Y. S. Mohamed and Wael A. Al-Tabey, Department of Mechanical Engineering, Faculty of Engineering, Alexandria University, Alexandria (21544), Egypt.*
- *Wael A. Al-Tabey,Department of Mechanical Engineering, Faculty of Engineering, Alexandria University, Alexandria (21544), Egypt. PH-00201007661514. E-mail: wael.altabey@yahoo.com*

For ductile matrices, the fatigue process is similar to that in metals in the sense that it consists of two stages: crack initiation and crack propagation. In fiber-reinforced polymers, the matrix is subjected to strain-controlled fatigue due to the constraint provided by the fibers. Table (1) shows the well-known failure criteria for orthotropic materials under plane stress state [2].

The applicability of a particular failure criterion depends on the material studied being ductile or brittle. Tsai-Hill criteria is suitable for glass-epoxy, other composites might be better treated with the maximum stress or the maximum strain criterion or even some other criteria [1]. But, in general, it is important to notice that the term ($\sigma_1\sigma_2$) has different coefficients in the different failure criteria; and, it is mainly, the coefficient of this term that adjusts the criterion to the experimental results [2].

2. experimental work

2.1 Testing machine

The used testing machine was designed by M. N. Abouelwafa et al [9] and used by other researcher in similar works [2, 3-8], then modifying this designe in new testing machine by Y. S. Mohamed [10], the important modification to the testing machine is adding hydraulic circuit to study the effect of internal hydrostatic pressure. The general layout of testing machine and hydraulic circuit is shown in Fig.1 and Fig.2, respectevely.

The testing machine is a strain controlled, rotating at constant speed of 380 rpm (6.33Hz), and capable of performing three different fatigue loading systems and hydrostatic pressure load.

The load systems are independent, and have the facility to apply different stresses. The specimen is subjected to a uniform load, along its whole length, through a gripping system consisting of two halves that enclose the specimen in between. The applied moment was measured via a load cell,fixed on the grippers, consisting of four active strain gauges, forming a full bridge. The signal is amplified and displayed on an oscilloscope and the whole system was calibrated.

The objective of hydraulic circuit is to obtain constant pressure inside the specimen and can be controlled by increasing or decreasing by controlling the flow control valve, the system records the change in internal pressure by Pressure transducer, until the specimen fails. The pressure transducer was calibrated and checked it on zero bars and the specimen was considered to have failed, when the pressure transducer reading falls down from its highest value.

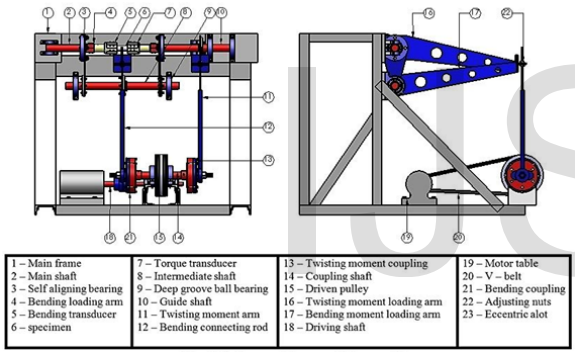

Fig.1.The general layout of testing machine

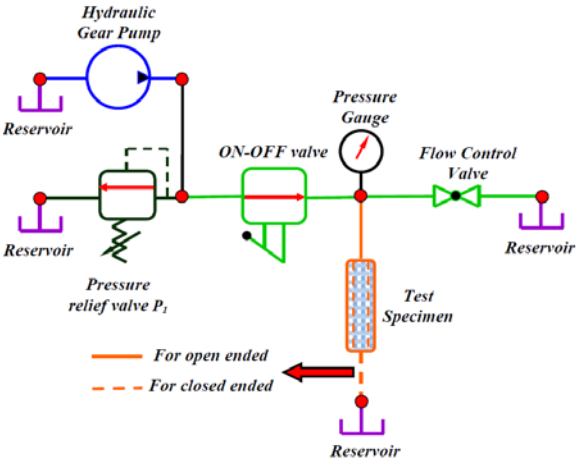

Fig.2. The general layout of hydraulic circuit

2.2 Test Fixtures

For the application of internal pressure efficiently, the specimen should be fixed properly to the test apparatus. The fixation should be strong enough to avoid leakage of test fluid, fracture or slip of the specimen at the matching region. The closure system should be guaranteed that uniform stresses are obtained through the test section cover the constraint on the test specimen in axial direction for closed end test. Accordingly, the specimens are fixed to the test system by means of the gripping end closure unit for this test, which is presented in Fig.3. The thickness of the tube ends were built up by additional layer of rubber tube to avoid gripping problems.

2.3 Specimens

Thick-walled tubes made from three layers of woven-roving E-glass/Epoxy with two fiber orientations,$[0^o,90^o]_{3s}$and $[\pm 45^o]_{3s}$, were used . There are two manufacture methods will be applied in this work to prepare the test specimens, in the first method (old method) M_1 the test specimens will be prepared by molding all layers around the mandrel in one step then the epoxy resin will be poured-on-it, then leave it to cure, and the new method M_2 will be discussed in this work, the test specimens will be prepared by molding first layer only around the mandrel then the epoxy resin will be poured - on-it, then leave to cure, and repeat previous step for the second layer and so on (i.e. as compound tubes).

A fiber volume fraction (V_f) ranging from 55 % to 65 % for method M_1. This range was used in previous works [2, 3-9], from 56% to 67% for method M_2, and has proved its suitability to ensure good adhesion between fibers and matrix, good strength and acceptable mechanical properties. Table (2) shows the properties of the used materials. Fig.4 shows the nominal dimensions of the used specimens, which were measured after complete curing.

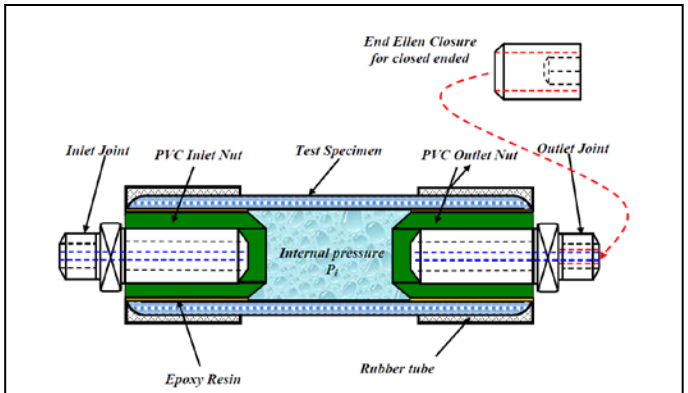

Fig.3. Schematic of Specimen closure system

TABLE 1
FAILURE CRITERIA / THEORIES OF FAILURE

No.	Name	Mathematical formula
1	Max. stress	$\sigma_1 = F_1\,,\quad \sigma_2 = F_2,\quad \sigma_6 = F_6$
2	Max. strain	$\sigma_1 = F_1 + \upsilon_{12}\sigma_2\,,\quad \sigma_2 = F_2 + \upsilon_{12}\frac{E_2}{E_1}\sigma_1,\quad \sigma_6 = F_6$
3	Hill criterion	$\left(\frac{\sigma_1}{F_1}\right)^2 - \left(\frac{1}{{F_1}^2} + \frac{1}{{F_2}^2}\right)\sigma_1\sigma_2 + \left(\frac{\sigma_2}{F_2}\right)^2 + \left(\frac{\sigma_6}{F_6}\right)^2 = 1$
4	Tsai-Hill	$\left(\frac{\sigma_1}{F_1}\right)^2 - \left(\frac{\sigma_1\sigma_2}{{F_1}^2}\right) + \left(\frac{\sigma_2}{F_2}\right)^2 + \left(\frac{\sigma_6}{F_6}\right)^2 = 1$
5	Norris interaction	$\left(\frac{\sigma_1}{F_1}\right)^2 + \left(\frac{\sigma_2}{F_2}\right)^2 + \left(\frac{\sigma_6}{F_6}\right)^2 = 1$
6	Norris distortional energy	$\left(\frac{\sigma_1}{F_1}\right)^2 - \left(\frac{\sigma_1\sigma_2}{F_1F_2}\right) + \left(\frac{\sigma_2}{F_2}\right)^2 + \left(\frac{\sigma_6}{F_6}\right)^2 = 1 \quad \text{or} \left(\frac{\sigma_1}{F_1}\right)^2 = 1 \quad \text{or} \left(\frac{\sigma_2}{F_2}\right)^2 = 1$
7	Hoffman	$\left(\frac{{\sigma_1}^2 - \sigma_1\sigma_2}{F_{1t}F_{1c}}\right) + \left(\frac{{\sigma_2}^2}{F_{2t}F_{2c}}\right) + \left(\frac{F_{1c} - F_{1t}}{F_{1t}F_{1c}}\right)\sigma_1 + \left(\frac{F_{2c} - F_{2t}}{F_{2t}F_{2c}}\right)\sigma_2 + \left(\frac{\sigma_6}{F_6}\right)^2 = 1$
8	Modified Marin	$\left(\frac{{\sigma_1}^2 - K_2\sigma_1\sigma_2}{F_{1t}F_{1c}}\right) + \left(\frac{{\sigma_2}^2}{F_{2t}F_{2c}}\right) + \left(\frac{F_{1c} - F_{1t}}{F_{1t}F_{1c}}\right)\sigma_1 + \left(\frac{F_{2c} - F_{2t}}{F_{2t}F_{2c}}\right)\sigma_2 + \left(\frac{\sigma_6}{F_6}\right)^2 = 1$ Where: K_2 is floating constant.
9	Tsai-Wu	$\left(\frac{1}{F_{1t}} - \frac{1}{F_{1c}}\right)\sigma_1 + \left(\frac{1}{F_{2t}} - \frac{1}{F_{2c}}\right)\sigma_2 + \left(\frac{{\sigma_1}^2}{F_{1t}F_{1c}}\right) + \left(\frac{{\sigma_2}^2}{F_{2t}F_{2c}}\right) + (2H_{12}\sigma_1\sigma_2) + \left(\frac{\sigma_6}{F_6}\right)^2 = 1$ And the following condition must be fulfilled, for stability: $\frac{1}{F_{1t}F_{1c}F_{2t}F_{2c}} - {H_{12}}^2 \geq 0$
10	Ashkenazi	$\left(\frac{\sigma_1}{F_1}\right)^2 + \left(\frac{\sigma_2}{F_2}\right)^2 + \left(\frac{\sigma_6}{F_6}\right)^2 + (2F_{12}\sigma_1\sigma_2) = 1$ $F_{12} = 0.5\left(\frac{4}{{\sigma_X}^2} - \frac{1}{{F_1}^2} - \frac{1}{{F_2}^2} - \frac{1}{{F_6}^2}\right)$ Where: σ_X is the global stress of 45° in tension.
11	Tsai-Hahn	The same formula as Tsai-Wu but H_{12} takes the form: $H_{12} = -0.5\sqrt{\frac{1}{F_{1t}F_{1c}F_{2t}F_{2c}}}$
12	Cowin	The same formula as Tsai-Wu but H_{12} takes the form: $H_{12} = \sqrt{\frac{1}{F_{1t}F_{1c}F_{2t}F_{2c}}} - \frac{1}{2{F_6}^2}$
13	Fischer	$\left(\frac{\sigma_1}{F_1}\right)^2 - C\left(\frac{\sigma_1\sigma_2}{{F_1}^2}\right) + \left(\frac{\sigma_2}{F_2}\right)^2 + \left(\frac{\sigma_6}{F_6}\right)^2 = 1$ Where: $k = \frac{E_1(1+\upsilon_{21}) + E_2(1+\upsilon_{12})}{2\sqrt{E_1E_2(1+\upsilon_{21})(1+\upsilon_{12})}}$

Where:

σ_1 and σ_2 are the local stress components in directions (1) and (2), respectively.
σ_6 is the local shear component.
F_{1t}&F_{1c} and F_{2t}&F_{2c} are the local tension and compression strength components in directions (1) and (2), respectively.
F_6 is the local shear strength component.
υ_{12} and υ_{21} represent Poisson's ratios in the local directions.
E_1 and E_2 are the local modullii of elasticity in directions (1) and (2), respectively.

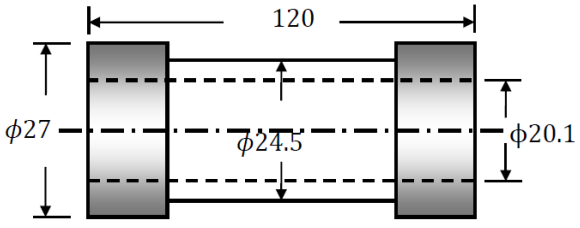

Fig.4. Nominal dimensions [mm] ± 0.1 mm

TABLE 2
PROPERTIES OF USED MATERIALS

Property	Woven-roving E-glass fibers	Epoxy Resin
Density	2551 kg/m³	1800 kg/m³
Modulus of elasticity	E = 76 GPa	E = 3.6 GPa
Poisson's ratio	ν = 0.37	ν = 0.35
Tensile strength	3.45 GPa	0.25 GPa

2.4 Stress state

Specimens are subjected to combined bending fatigue moments and internal Pressure with different pressure values. Being closed end cylindrical in shape, their global stress(σ_x), (σ_y) and (τ_{xy}) may be found from the following equation:

$$\sigma_x = \frac{My}{I} + \sigma_l,\ \sigma_y = \sigma_H \text{ and } \tau_{xy} = 0$$

Where:

M : applied bending moment $(M = M_m + M_a \sin(\omega t))$.

M_m and M_a: mean and amplitude bending moments, respectively.

I: second moment of area for tube; $I = (\pi/64)(d_o^4 - d_i^4)$.

σ_l: Longitudinal stress (MPa), $(\sigma_l = P_i r_i^2/{r_o}^2 - r_i^2)$for thick tube.

σ_H: Hoop stress (MPa),$\left(\sigma_H = (P_i r_i^2/{r_o}^2 - r_i^2)(1 + {r_o}^2/r^2)\right)$for thick tube.

P_i : Internal pressure.

d_o and d_i : Outer and inner diameters of the specimen, respectively and $r = d_i/2$.

The $[0^o,90^o]_{3s}$ specimens had a pure local stress state, $\sigma_1 = \sigma_x$, $\sigma_2 = \sigma_y$and $\sigma_6 = 0$, while the $[\pm 45°]_{3s}$ specimens had local stress state, $\sigma_1 = \sigma_2 = (1/2)(\sigma_x + \sigma_y)$and $\sigma_6 = (1/2)(\sigma_x - \sigma_y)$.

3. Selected failure criteria

Working with failure criteria were done through three steps; first, selecting some of the known failure criteria suitable to be used for the present material, second, reforming them according to the local stress components, for both fiber orientations. Finally, the most suitable criteria for each orientation will be selected, checked and modified if required.

Many previous works had been done considering the suitability of failure criteria to the present investigated materials. Considering these works [2, 3-9, 11-13] it was found that the most widely used and suitable criteria for GFRP under different loading conditions were the following six criteria:

1-Norris interaction, 2-Norris distortional,
3-Tsai – Hahm, 4- Hill,
5-Tsai – Hill, 6- Tsai – Wu.

Using the local stress components of both the $[\pm 45°]_{3s}$ and the $[0,90°]_{3s}$ specimens to substitute in the selected six criteria has shown that all failure criteria have the four forms for the $[0,90°]_{3s}$and $[\pm 45°]_{3s}$specimens, as shown in table (3)

TABLE 3
SELECTED FAILURE CRITERIA FOR $[0, 90°]_{3S}$ AND $[\pm 45°]_{3S}$ SPECIMENS SUBJECTED TO COMBINED COMPLETELY REVERSED PURE BENDING AND INTERNAL PRESSURE STRESSES

Failure criteria	$[0,90°]_{3s}$ specimens	$[\pm 45°]_{3s}$ specimens
Hill	$\left(\frac{\sigma_1}{F_1}\right)^2 + \left(\frac{\sigma_2}{F_2}\right)^2 - 2\left(\frac{\sigma_1\sigma_2}{F_1F_2}\right) = 1$	$\left(\frac{\sigma_6}{F_6}\right)^2 = 1$
Tsai-Hill, Norris distortional & Tsai-Hahn	$\left(\frac{\sigma_1}{F_1}\right)^2 + \left(\frac{\sigma_2}{F_2}\right)^2 - \left(\frac{\sigma_1\sigma_2}{F_1F_2}\right) = 1$	$\left(\frac{\sigma_1}{F_1}\right)^2 + \left(\frac{\sigma_6}{F_6}\right)^2 = 1$
Tsai-Wu	$\left(\frac{\sigma_1}{F_1}\right)^2 + \left(\frac{\sigma_2}{F_2}\right)^2 + 2\left(\frac{\sigma_1\sigma_2}{F_1F_2}\right) = 1$	$4\left(\frac{\sigma_1}{F_1}\right)^2 + \left(\frac{\sigma_6}{F_6}\right)^2 = 1$
Norris interaction	$\left(\frac{\sigma_1}{F_1}\right)^2 + \left(\frac{\sigma_2}{F_2}\right)^2 = 1$	$2\left(\frac{\sigma_1}{F_1}\right) + \left(\frac{\sigma_6}{F_6}\right)^2 = 1$

4. test results

It is important to note that, in order to avoid any misleading data, only the specimens that had their failure features within the accepted gauge section, the middle third of the whole length were considered; while those that have their failure due to any gripping problems were excluded.

4.1 Static tests

4.1.1 Static Bending and Torsion tests

Static bending and torsion tests were performed on the tubular specimens of both orientations, $[0^o,90^o]_{3s}$ and $[\pm 45°]_{3s}$, and two manufacture methods M_1 and M_2, in order to find out their ultimate global bending strengths (S_u) and ultimate global shear strengths (S_{us}),It should be noted that, the local static strength in the fiber direction (F_{1s}) is equal to

the static bending strength, and the local static shear strength (F_{6s}) is equal to the ultimate global shear strength [2, 5, 8, 14].Which was found to be as follows:

- (S_u) of the M_1,$[0^o,90^o]_{3s}$ specimens = 182 MPa
- (S_u) of the M_2, $[0^o,90^o]_{3s}$ specimens = 198MPa
- (S_u) of the M_1,$[\pm45°]_{3s}$ specimens = 159 MPa
- (S_u) of the M_2, $[\pm45°]_{3s}$ specimens = 173MPa
- (S_{us}) of the M_1, $[0^o,90^o]_{3s}$ specimens = 69.5 MPa
- (S_{us}) of the M_2, $[0^o,90^o]_{3s}$ specimens = 24 MPa
- (S_{us}) of the M_1, $[\pm45°]_{3s}$ specimens = 84 MPa
- (S_{us}) of the M_2, $[\pm45°]_{3s}$ specimens = 35 MPa

4.2 Fatigue tests

All specimens were tested under ambient conditions and constant frequency of 6.33 Hz. The data points were used to plot the corresponding S-N curves on a semi-log scale, being fitted using the power law: $maximumstress = aN^b$, representing the bending fatigue strength (S_f). Failure was considered to occur when the load reading decreased by about 20% of its original value. In other words, 20 % reduction in the strength of the specimen will represent failure.

4.2.1 Pure Bending and pure Torsion fatigue test

Both fiber orientations, $[0^o,90^o]_{3s}$ and $[\pm45°]_{3s}$, with twomanufacture methodsM_1andM_2 were tested under completely reversed pure bending and pure torsion, in order to find out their bending and torsion fatigue strength (S_f) and (S_{fs}) which also represents the local fatigue strength in the fibre direction (F_{1f}) and (F_{6f}), [2, 3-8, 14]. The corresponding power equation was:

- $\sigma_{max} = 314.3N^{-0.1361}$For the M_1, $[0^o,90^o]_{3s}$
- $\sigma_{max} = 484.4N^{-0.1612}$For the M_2, $[0^o,90^o]_{3s}$
- $\sigma_{max} = 226.6N^{-0.1284}$For the M_1, $[\pm45°]_{3s}$
- $\sigma_{max} = 397.2N^{-0.1514}$For the M_2, $[\pm45°]_{3s}$
- $\tau_{max} = 93.79N^{-0.1416}$For the M_1, $[0^o,90^o]_{3s}$
- $\tau_{max} = 48.36N^{-0.1612}$For the M_2, $[0^o,90^o]_{3s}$
- $\tau_{max} = 121.3N^{-0.1115}$For the M_1, $[\pm45°]_{3s}$
- $\tau_{max} = 73.16N^{-0.184}$For the M_2, $[\pm45°]_{3s}$

4.2.2 Combined completely reversed Bending and internal pressure fatigue test

Tests were performed on both fiber orientations, $[0^o,90^o]_{3s}$ and $[\pm45°]_{3s}$, at four different pressure ratios $P_r = 0, 0.25, 0.5, 0.75$(i.e. pressures amounting to 0%, 25%, 50% and 75% of the burst pressure). Fig.5 and Fig.6 show the corresponding S-N curves at all pressure ratios for both fiber orientations. The two constants (a) and (b) were found to have the values given in Table (4) and Table (5) .

TABLE 4
FATIGUE CONSTANTS (a) AND (b) FOR $[0°,90°]_{3S}$ SPECIMENS

Pressure ratio (P_r)	$[0,90°]_{3s}$		
	a (MPa)	*b*	*Correlation factor*
0	*314.3*	*-0.1361*	*0.9926*
0.25	*242.5*	*-0.1359*	*0.9858*
0.5	*163.2*	*-0.133*	*0.9837*
0.75	*99.88*	*-0.1305*	*0.9811*

TABLE 5
FATIGUE CONSTANTS (a) AND (b) FOR $[\pm45°]_{3S}$ SPECIMENS

Pressure ratio (P_r)	$[\pm45°]_{3s}$		
	a (MPa)	*b*	*Correlation factor*
0	*226.6*	*-0.1284*	*0.9953*
0.25	*169.7*	*-0.1264*	*0.9876*
0.5	*107.5*	*-0.1218*	*0.9845*
0.75	*62.09*	*-0.1181*	*0.9803*

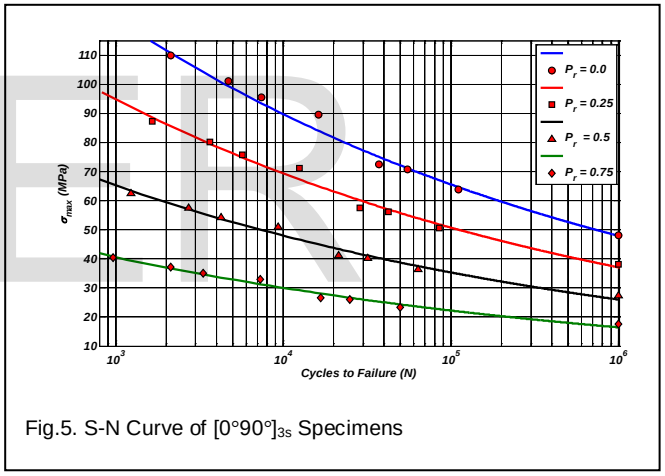

Fig.5. S-N Curve of $[0°90°]_{3s}$ Specimens

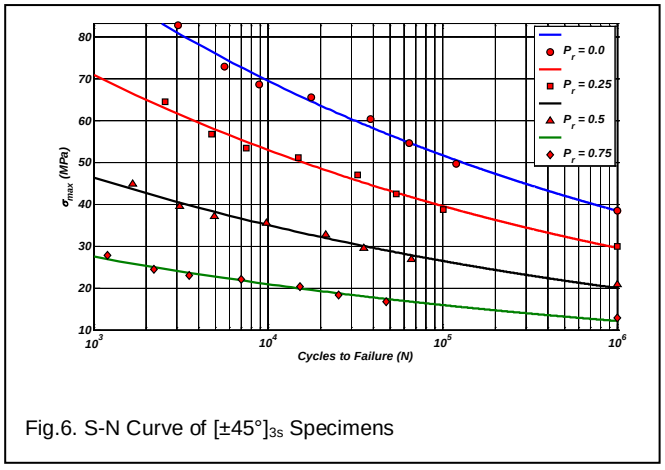

Fig.6. S-N Curve of $[\pm45°]_{3s}$ Specimens

5. Analysis and discussion

5.1 Applicability of failure criteria

To evaluate the validity of the failure criteria, we shall the right hand side of the equations representing the failure criteria as a relative damage. The relation between the relative damage (R.D.) with the number of cycles to failure (N) is constructed for different criteria. In these curves as much as they are close to unity, this means the validity of particular criterion to the test conditions. If it less than unity, then the criterion is predicting a specimen life more than the actual life of the experiment.

5.1.1 The relative damage for $[0,90°]_{3s}$ specimens

The relative damage (R.D.) were calculated according to selected suitable failure criteria presented in Table (3), for the $[0,90°]_{3s}$ specimens under completely reversed pure bending, completely reversed pure torsion and combined pressure and completely reversed bending fatigue loading with two methods of manufacturing M_1 and M_2 and different pressure ratio $(P_r = 0, 0.25, 0.5, 0.75)$. Fig.7andFig.8 shows the relative damage for the $[0,90°]_{3s}$ specimens against the number of cycles to failure. The values of (R.D.) are far from unity. This main that, the available different failure criteria are not suitable under these conditions and must be modified to best suit the studied case.

5.1.2 The relative damage for [±45°]3s specimens

Fig.9 and Fig.10 represent the relative damage for the $[\pm 45°]_{3s}$ specimens under completely reversed pure bending, completely reversed pure torsion and combined pressure and completely reversed bending fatigue loading with two methods of manufacturing M_1 and M_2 and different pressure ratio $(P_r = 0, 0.25, 0.5, 0.75)$ against the number of cycles to failure. From these Figures, it can be noticed that these failure criteria are not valid and must be modified.

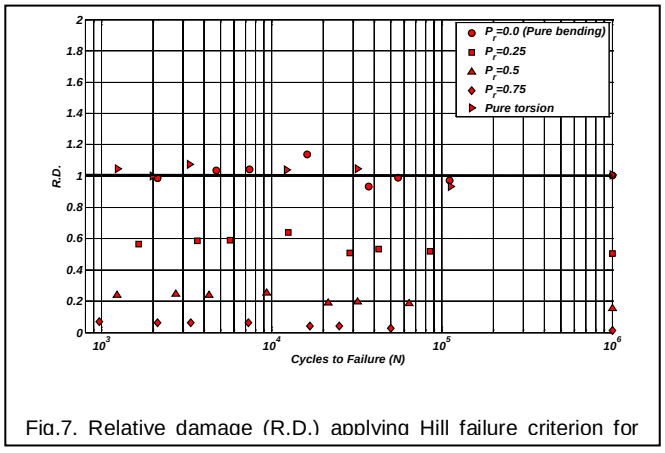

Fig.7. Relative damage (R.D.) applying Hill failure criterion for

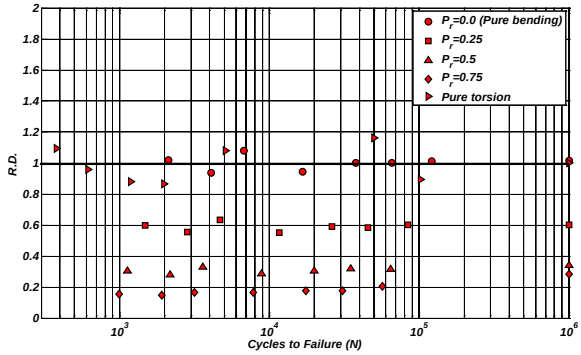

Fig.8.Relative damage (R.D.) applying Tsai-Hahn failure criterion for the M_2, $[0,90°]_{3s}$ specimens

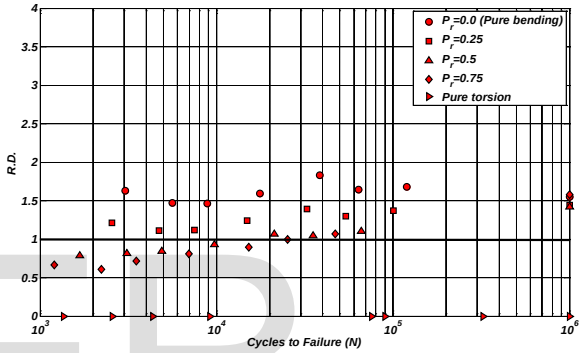

Fig.9. Relative damage (R.D.) applying Tsai-Wu failure criterion for the M_1, $[\pm 45°]_{3s}$ specimens

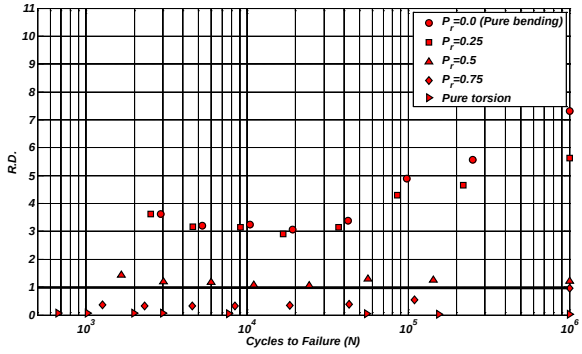

Fig.10. Relative damage (R.D.) applying Norris & Mckinnon failure criterion for the M_2, $[\pm 45°]_{3s}$ specimens

5.1.3 Modification of Failure Criteria

Choosing the suitable failure criterion represents the main target for many researchers working with materials, and it represents the first step for new materials before being used in the field. Considering composite materials, specifically, makes it more challenging, because of their very special behavior and characteristics. Besides, it must be noted that, the suitability of a certain criterion differs greatly according

to the tested material, and its stress state. All failure criteria have their right hand side to be unity, and their left hand side contains the local stress components divided by their corresponding strengths. Therefore, the left hand side of any criterion was named to be its Relative Damage (R.D.) Secondly, a comparison was conducted for the value of the R.D. to unity, the criterion is suitable if its R.D. has a value near unity.

From the previous Figures 7 to 10, it is noted that; the relative damage R.D. values calculated from Tsai-Wu criterion at pure torsion for $[\pm 45°]_{3s}$ are equal zero. Therefore, we excluded it from our work; i.e. it is not suitable for the present case. On other hand, all remaining theories of failure have very small values of R.D. for all pressure ratios P_r and for both manufacturing method M_1 and $M_2$with all fiber orientation accept fiber orientation $[\pm 45°]_{3s}$in method M_2 only for all pressure ratios P_r, they have the values of R.D. far from unity. This may be explained by considering the drop in the values of ultimate global shear strengths (S_{us}), and local stresses due to the delamination failure mode during torsional tests of specimens from method M_2, but this reason is not appear in values of R.D. for fiber orientation $[0,90°]_{3s}$because, it has local stress σ_6 equal zero for all pressure ratio P_r.

Taking from the previous works of [2,3-8]in to consideration, it is obvious that, the Tsai-Hahn is more suitable failure criteria for the tension-compression stress state and it may be modified to best suit the present work; i.e. making the R.D.

Consequently, a new procedure was proposed for adapting these two criteria to best fit the tested case. The suggested procedure was based mainly on introducing a new term to increase the correlation between the experimental data and the theoretical equations.

The main principals for selecting the new term:

1. It must reflect the effect of both, hoop and amplitude stress components.
2. It must depend on the local stress and strength components and not the global ones.
3. It should contain a minimum number of variables, as possible, for simplicity and ease of use.
4. It must be dimensionless.

From the previous principals had led us to suggest introducing the forms of failure criterion:

$$\left(\frac{\sigma_1}{F_1}\right)^2+\left(\frac{\sigma_2}{F_2}\right)^2+\left(\frac{\sigma_6}{F_6}\right)^2-\left(\frac{\sigma_1\sigma_2}{F_1F_2}\right)+W_1=1$$

(For all pressure ratios P_r and for both manufacturing method M_1 and $M_2$with all fiber orientation accept fiber orientation $[\pm 45°]_{3s}$ in method M_2 only for all pressure ratios P_r) and

$$\left(\frac{\sigma_1}{F_1}\right)^2+\left(\frac{\sigma_2}{F_2}\right)^2+W_2\left(\frac{\sigma_6}{F_6}\right)^2-\left(\frac{\sigma_1\sigma_2}{F_1F_2}\right)+W_1=1$$

(For fiber orientation $[\pm 45°]_{3s}$ in method M_2 only for all pressure ratios P_r).

Where:

$$W_1=\frac{\left[\sigma_{H_{max}}\right]_{[\theta,M]}}{a_{[\theta,M]}}+P_r+\left[\left(V_f\right)_{avrg}\right]_{[\theta,M]}$$

$$W_2=[\theta]^{P_r}\left(\frac{[\tau_{max}]^{1/3}_{[\pm 45°,M_2]}}{[S_{us}]_{[\pm 45°,M_2]}}\right)$$

$\left[\sigma_{H_{max}}\right]_{[\theta,M]}$: The maximum hoop stress corresponding to its fiber orientations and manufacturing method.

$a_{[\theta,M]}$: The fatigue constant a corresponding to its fiber orientations and manufacturing method

P_r: Pressure ratio.

$\left[\left(V_f\right)_{avrg}\right]_{[\theta,M]}$: The average volume fraction a corresponding to its fiber orientations and manufacturing method.

θ: Fiber orientation angle in rad.

$[S_{us}]_{[\pm 45°,M_2]}$: Ultimate global shear strengths corresponding to fiber orientation $[\pm 45°]_{3s}$ and manufacturing. Method M_2.

$[\tau_{max}]_{[\pm 45°,M_2]}$: The shear strength of specimen corresponding to fiber orientation $[\pm 45°]_{3s}$ and manufacturing. Method M_2.

The values of R.D. after modification, according to the new failure criteria, were plotted against the number of cycles to failure under both manufacturing method M_1 and $M_2$for all fiber orientations accept fiber orientation $[\pm 45°]_{3s}$in method M_2 only as shown in Fig.11 and for fiber orientation $[\pm 45°]_{3s}$in method M_2 only in Fig.12 respectively.

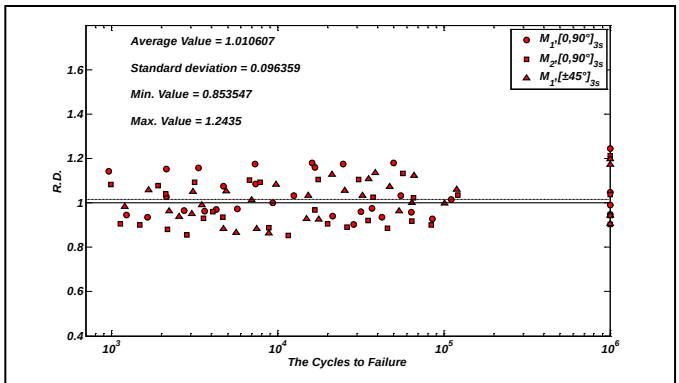

Fig.11. Relative damage (R.D.) applying present failure criterion for both manufacturing method M_1 and M_2 for all fiber orientations accept fiber orientation $[\pm 45°]_{3s}$ in method M_2

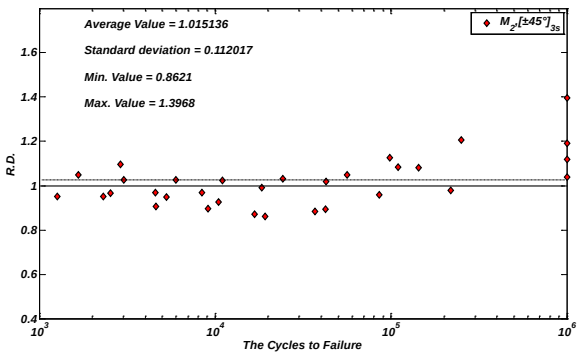

Fig.12. Relative damage (R.D.) applying present failure criterion for fiber orientation $[\pm 45°]_{3s}$ in method M_2

6. Conclusions

Fig.11and Fig.12shows that the modifying criterion gives excellent results for both manufacturing method M_1 and $M_2$for all fiber orientations and for all pressure ratios, where, the values of R.D. are around the theoretical value of unity. For both manufacturing method M_1 and $M_2$for all fiber orientations accept fiber orientation $[\pm 45°]_{3s}$in method M_2, Fig.11, the R.D. are ranging from 0.853547 as a minimum value to 1.2435 as a maximum value with an average value of 1.010607 and standard deviation of 0.096359, and for fiber orientation $[\pm 45°]_{3s}$in method M_2, Fig.12, are ranging from 0.8621 as a minimum value to 1.3968 as a maximum value with an average value of 1.015136 and standard deviation of 0.112017, which are very near to unity , and the difference may be referred to scatter in experimental data.

REFERENCES

[1] F. James, Introduction to Materials Science for Engineers, Maxwell Macmillan (1985).
[2] A.A. El-Midany, Fatigue of Woven-Roving Glass Fibre Reinforced Polyester under Combined Bending and Torsion, PhD. Thesis, Alexandria University – Egypt
[3] Mohamed N. A., The Effect of Mean Stress on the Fatigue Behaviour of Woven-Roving GFRP Subjected to Torsional Moments, MSc. Thesis, Alexandria University, Egypt, 2002.
[4] Mohamed M. Y., The Inclusion Effect on the Fatigue Behaviour of Woven-Roving GRP Composite Materials , MSc. Thesis, Alexandria University, Egypt, 2001.
[5] Mustafa M. E., Fatigue Behaviour of Woven-Roving GFRP Under Combined Bending and Torsion Moments with Different Fluctuating Stresses, MSc. Thesis, Alexandria University, Egypt, 2006.
[6] Sharara A. I., Effect of Stress Ratio on Fatigue Characteristics of Woven-Roving Glass Reinforced Polyester, MSc. Thesis, Alexandria University, Egypt, 1997.
[7] Mustafa M. E., Fatigue Behaviour of Woven-Roving Glass Reinforced Polyester Under Combined Out-of-Phase Bending and Torsion Moments with Different Fluctuating Stresses, PhD. Thesis, Alexandria University, Egypt, 2011.
[8] Y. S. Mohamed, A Study the Effect of Fiber Orientation and Negative or Positive Stress Ratios on Fatigue Characteristics of Woven-Roving Glass Reinforced Polyester Under Combined Bending and Torsional Moments, PhD. Thesis, Alexandria University, Egypt, 2011.
[9] M. N. Abouelwafa, Hamdy A. H. and Showaib E. A., A New Testing Machine for Fatigue Under Combined Bending and Torsion Acting Out-of-Phase, Alexandria Engineering Journal, Vol.28, No.4, Pp.113-95, 1996.
[10] Y. S. Mohamed and Graduation project groups, Composite Materials, Fatigue Testing and Molding Machines, Graduation Project, Mechanical Engineering Department, Alexandria University, Alexandria, Egypt.
[11] M.J. Owen, and J.R. Griffiths, Evaluation of Biaxial Stress Failure for a GFRP Under Static and Fatigue Loading, J. of Material Science, Vol. 13, pp. 1521- 1537 (1978).
[12] M.J Owen and D.J. Grice, Biaxial Strength Behaviour of Glass Fabric- Reinforced Polyester Resins, J. of Composite Materials, pp. 13-25 (1981).
[13] A. Sadao and T. Adachi, Non-linear Stress-Strain Response of laminated Composites, J. of Composite Materials, Vol. 13, pp. 206-217 (1979).
[14] A.K. Jihad, "Delamination Growth of GFRE Composites under Cyclic Torsional Moments", PhD. Thesis, Alexandria University – Egypt (2001).